Published in final edited form as:
*Immunity*. 2007 February ; 26(2): 215–226. doi:10.1016/j.immuni.2006.12.005.

# Heat Shock Protein gp96 Is a Master Chaperone for Toll-like Receptors and Is Important in the Innate Function of Macrophages

**Yi Yang**[1], **Bei Liu**[1], **Jie Dai**[1], **Pramod K. Srivastava**[1], **David J. Zammit**[1], **Leo Lefrançois**[1], and **Zihai Li**[1,*]

[1] Department of Immunology, MC 1601, University of Connecticut School of Medicine, Farmington, CT 06030, USA

## SUMMARY

gp96 is an endoplasmic reticulum chaperone for cell-surface Toll-like receptors (TLRs). Little is known about its roles in chaperoning other TLRs or in the biology of macrophage in vivo. We generated a macrophage-specific gp96-deficient mouse. Despite normal development and activation by interferon-γ, tumor necrosis factor-α, and interleukin-1β, the mutant macrophages failed to respond to ligands of both cell-surface and intracellular TLRs including TLR2, TLR4, TLR5, TLR7, and TLR9. Furthermore, we found that TLR4 and TLR9 preferentially interacted with a super-glycosylated gp96 species. The categorical loss of TLRs in gp96-deficient macrophages operationally created a conditional and cell-specific TLR null mouse. These mice were resistant to endotoxin shock but were highly susceptible to *Listeria monocytogenes*. Our results demonstrate that gp96 is the master chaperone for TLRs and that macrophages, but not other myeloid cells, are the dominant source of proinflammatory cytokines during endotoxemia and *Listeria* infections.

## INTRODUCTION

Multicellular organisms have evolved to defend against microbes by expressing pattern-recognition receptors (PRRs) such as Toll-like receptors (TLRs) to recognize unique structural entities of these pathogens. TLRs are germline-encoded PRRs that sense pathogen-associated molecular patterns (PAMPs) (Iwasaki and Medzhitov, 2004). There are 12 functional murine TLRs (Roach et al., 2005; Takeda and Akira, 2005) that localize subcellularly either on the cell surface or in intracellular vesicular compartments. Although TLRs can be expressed in nonimmune cells, the highest expression is generally on professional antigen-presenting cells (APCs) such as dendritic cells (DCs) or macrophages (Mϕ), indicating the critical roles of TLR signaling in the function of APCs, which include the production of proinflammatory cytokines, T helper 1 (Th1) polarization (Schnare et al., 2001), modulation of regulatory T cells (Bettelli et al., 2006; Pasare and Medzhitov, 2003, 2004), and ultimately the priming of the adaptive immune response.

Signaling via TLRs is regulated by both positive and negative factors (Akira and Takeda, 2004). TLR4, for example, transmits signals via at least four cytosolic adaptor molecules



*Correspondence: zli@up.uchc.edu.

Supplemental Data Five Supplemental Figures can be found with this article online at http://www.immunity.com/cgi/content/full/26/2/215/DC1/.

(O'Neill et al., 2003) including MyD88, TIRAP, TRIF, and TRAM. In contrast, LPS signaling via TLR4 can be negatively regulated by a number of factors (Liew et al., 2005) including IRAK-M, TRAIL-R, A20, SOCS1, SIGIRR, and Fliih (Wang et al., 2006). Moreover, TLR function can also be regulated at gene and protein levels, exemplified by somatic mutations of the *Tlr5* (Hawn et al., 2005), ubiquitin-dependent degradation of TLR2 and TLR9 by binding to TRIAD3A (Chuang and Ulevitch, 2004), and the dependence on gp96 for the folding and export of TLR1, TLR2, and TLR4 (Randow and Seed, 2001).

gp96 (Srivastava et al., 1986), also known as grp94 (Lee et al., 1981), endoplasmin, and ERp99, is an endoplasmic reticulum (ER) paralog of heat shock protein 90 (HSP90) (Yang and Li, 2005). Like other HSPs, gp96 is induced by the accumulation of misfolded proteins (Kozutsumi et al., 1988); it binds and hydrolyzes ATP (Li and Srivastava, 1993) and chaperones multiple protein substrates including immunogloblulin (Ig) chains (Melnick et al., 1994). Consistent with the roles of gp96 as a “housekeeping” molecule, gp96-deficient murine embryos do not survive beyond 5.5 days (Stoilova et al., 2000). Surprisingly, gp96 is able to rescue the loss of cell-surface TLR1, TLR2, and TLR4 in a mutant pre-B cell line that expresses only a truncated gp96 because of insertional mutagenesis (Randow and Seed, 2001), demonstrating the nonessential role of gp96 for cell viability but its unique chaperone function for cell-surface TLRs. However, it is unclear whether the functional integrity of gp96 is important for the folding of other TLRs such as TLR7 (Nishiya et al., 2005) and TLR9 (Barton et al., 2006; Latz et al., 2004), which are distributed in the endosome and ER, respectively, rather than on the cell surface.

In this study, we generated a conditional gp96-deficient mouse by first inserting a loxP sequence at each side of the first exon of gp96-encoding gene *Hsp90b1*, followed by crossing engineered mice with LysMcre mice, which had cre recombinase knocked in to the lysozyme M locus (Clausen et al., 1999). We found that the activity of the LysM-driven cre was mostly restricted to granulocytes, monocytes, and Mϕ, but not to DCs or lymphocytes, despite the presence of LysM activity in a small population of the hematopoietic stem cells (Ye et al., 2003). We demonstrated that gp96-deficient Mϕ developed normally and could be activated through the classic pathway with interferon-γ (IFN-γ) and tumor necrosis factor-α (TNF-α) as well as with interleukin-1β (IL-1β). More importantly, gp96 is essential for signaling via both cell-surface and intracellular TLRs including TLR2, TLR4, TLR5, TLR7, and TLR9; gp96 chaperoned TLR9 and TLR4 in a manner that was dependent on calcium and N-linked glycosylation. Further, Mϕ-specific gp96-deficient mice were highly susceptible to the acute infection by *Listeria monocytogenes* (LM), indicating the importance of Mϕ and TLR function in the clearance of this organism. However, these mice were resistant to septic shock induced by endotoxin. Our results demonstrate that gp96 is the unique and obligatory master chaperone for TLRs, and Mϕ are the dominant source of proinflammatory cytokines in vivo during endotoxemia and *Listeria* infection.

## RESULTS

### Generation of a Conditional and Mφ-Selective gp96-Deficient Mouse

To understand the roles of gp96 on the organismal level, we generated a conditional gp96-deficient mouse by flanking the first exon of *Hsp90b1* with one LoxP sequence at each side, named *Hsp90b1*$^{flox}$ (Figure 1A). Homologous recombination was confirmed by a Southern blot analysis (Figure 1B). By crossing *Hsp90b1*$^{flox}$ mice with EIIa-cre mice, which express cre under the adenovirus EIIa promoter (Lakso et al., 1996), we generated *Hsp90b1*$^{flox/–}$ mice that had one allele of *Hsp90b1* “floxed” and the other allele deleted via cre-mediated recombination (Figure 1B). In order to generate a Mϕ-specific gp96-deficient mouse, we took advantage of LysMcre mice that express cre in the myeloid lineages of the hematopoietic system (Clausen et al., 1999). Because the activity of LysMcre had not been

well characterized in DCs, we addressed the cell specificity of LysMcre activity by crossing LysMcre mice with Z/EG mice (Novak et al., 2000), which express the green fluorescence protein (GFP) reporter only after a cre-mediated excision of the floxed *lacZ* gene upstream of GFP. This step is important to accurately interpret our later in vivo data. Whereas no GFP was found in any cells of Z/EG mice (data not shown), we detected GFP selectively in $CD11b^{high}Gr\text{-}1^{high}$ and $CD11b^{high}Gr\text{-}1^{interm}$ populations in $LysMcre^{+}$ Z/EG mice (Figure 1C); GFP was completely absent in T, B, and NK cells, $CD11c^{+}$ DC, and plasmacytoid DC. We then generated $LysMcre^{+/-}$ $Hsp90b1^{flox/-}$ (abbreviated KO) mice by intercrossing $Hsp90b1^{flox/-}$ and LysMcre mice. The expression level of gp96 in various cells from KO and $LysMcre^{+/-}$ $Hsp90b1^{flox/WT}$ (abbreviated WT) mice was compared. Immunoblot (IB) revealed the marked reduction of gp96 in KO bone marrow-derived Mϕ (BMDM) by antibody (Ab) against the N-terminal (9G10), C-terminal (SPA-851), and multiple epitopes (67-12) of gp96; gp96 was deleted completely from KO peritoneal Mϕ (pMϕ) (Figure 1D). By intracellular staining, we found that the loss of gp96 was more severe in terminally differentiated pMϕ (99.9% reduction), followed by BMDM (89% reduction) and splenic monocytes/Mϕ (~40% reduction) (Figure 1E), which is expected because residual gp96 has to undergo normal slow turnover with $T_{1/2}$ of ~5 days (data not shown) after successful deletion of *Hsp90b1* gene. Consistent with the specificity of LysMcre (Figure 1C), gp96 expression was unaltered in DC, B, T, and NK cells (Figure 1F). The apparent normal expression of gp96 in $Gr\text{-}1^{+}$ cells, despite cre activity, was due to the combination of rapid turnover of granulocytes ($T_{1/2}$ < 1 day) and the long $T_{1/2}$ of gp96. Collectively, we have successfully generated a Mϕ-selective gp96-deficient mouse.

## Normal Hematopoiesis, Differentiation, and Cytokine-Mediated Activation of Mφ in $LysMcre^{+/-}$ $Hsp90b1^{flox/-}$ Mice

$LysMcre^{+/-}$ $Hsp90b1^{flox/-}$ mice were developmentally normal and fertile. Mice at the age of 6–8 weeks were analyzed for the relative distribution of immune cells in the peripheral blood and primary and secondary lymphoid organs (spleen and lymph nodes). No significant differences in the cellularity (data not shown) or distribution of major cellular components were found between WT and KO mice (Figures 2A and 2B), demonstrating that gp96 ablation in $LysM^{+}$ cells does not affect general hematopoiesis.

We also characterized the phenotype of DCs. In the murine spleen, there are at least four types of DC (Shortman and Liu, 2002) including plasmacytoid DC (expressing pDCA-1) and myeloid DC that bear $CD4^{+}CD8^{-}$, $CD4^{-}CD8^{+}$, and $CD4^{-}CD8^{-}$ cell-surface marker. We found that there were no major alterations in any of those DC subpopulations (Figure 2C). Additionally, we found no gross alteration of the architecture of the spleen by immunofluorescence microscopy after staining with Ab against B220, CD11b, and F4/80 (Figure 2D).

We next determined the impact of gp96 loss on the function of pMf. Both WT and KO mice have $F4/80^{+}$ Mϕ in the peritoneal exudates cells (PEC), which have identical forward-scattering and side-scattering profiles (data not shown) and are indistinguishable morphologically on light microscopy (Figure 2E). Like WT cells, gp96-deficient pMϕ can be activated by the combination of IFN-γ and TNF-α to produce nitric oxide (NO) (Figure 2F) and to upregulate cell-surface expression of MHC class II (Figure 2G) and class I molecules (data not shown). In addition, despite reduced expression of $\beta_2$ integrins, KO and WT BMDMs expressed the same amount of cell-surface MHC I, MHC II, CD14, CD16/32, CD43, CD44, CD80, CD86, and CD103 (see Figure S1 in the Supplemental Data available online). Thus, the differentiation of Mϕ is uncompromised, which was further confirmed by the similar density of F4/80-positive cells in nonlymphoid organs such as the liver by immunofluorescence microscopy (data not shown). Thus, there is no substantial compromise

in the hematopoiesis in LysMcre$^{+/-}$*Hsp90b1*$^{flox/-}$ mice; the differentiation and cytokine-mediated activation of Mϕ were independent of gp96.

## Loss of Responsiveness of gp96-Deficient Cells to the Ligands of Both Intracellular and Cell-Surface TLRs

We next focused our study on the impact of gp96 loss on TLR function, because gp96 has an established role in folding and cell-surface expression of TLR1, TLR2, and TLR4 (Randow and Seed, 2001). As expected, KO cells failed to produce IL-6 or TNF-α in response to 4 hr stimulations to Pam3CSK4 and LPS by intracellular staining (Figure 3A); the phenotype was not due to any defect in the common cytosolic pathway of Toll-IL-1 receptor (TIR) signaling, because gp96 is localized primarily in the ER lumen and does not have access to interact with cytosolic proteins. Further, gp96 KO pMϕ responded normally to IL-1β to produce a similar amount of IL-6 and TNF-α (Figure 3A).

TLRs are type I transmembrane proteins that contain conserved leucine-rich repeats (LRR) for ligand binding in the extracellular domains. As an ER luminal protein, gp96 might interact with the extracellular domains of other TLRs. We found indeed that KO but not WT pMϕ failed to respond to ligands for both TLR5 (flagellin) and TLR7 (R848) (Figure 3A). Similarly, gp96 KO BMDM secreted significantly less IL-6 and IL-12p40 in response to the ligand of TLR4 (LPS) and TLR9 (immunostimulatory CpG oligonucleotide) (Figure 3B). Of significance, WT but not KO pMϕ responded to CpG (Figure 3C) after IFN-γ priming. Unprimed pMϕ from both WT and KO mice failed to respond to CpG (data not shown). The dependency on IFN-γ ruled out the possibility that the CpG-activating activity was due to contamination by cell-surface TLR ligands such as LPS. As expected, pMϕ from TLR2 and TLR4 double deficient mice remained responsive to stimulations by CpG as well as R848 (Figure 3C). We then compared the amount of TNF-α released from pMϕ of WT, gp96 KO, and *Tlr2*$^{-/-}$*Tlr4*$^{-/-}$ mice to poly I:C stimulation, because the production of proinflammatory cytokines by pMϕ in response to poly I:C is mainly mediated by TLR3-Trif pathway (Gitlin et al., 2006). We found that TNF-α release was significantly reduced from gp96 KO cells in response to poly I:C (Figure S2), arguing that gp96 is important for TLR3 function as well.

We also obtained gp96 mutant pre-B cell line from Seed and colleagues (Randow and Seed, 2001) and examined WT as well as mutant pre-B cell lines (Figure 3D) for their responsiveness to TLR ligands. All cells expressed a NFκB-driven GFP reporter gene. Mutant cells failed to respond to LPS, lipoteichoic acid (LTA), R848, and CpG (Figure 3E); stable expression of gp96 in mutant cells restored its responsiveness to these TLR ligands (Figure 3E). Thus, gp96 is essential for the function of both cell-surface and intracellular TLRs, but not for IL-1, TNF-α, and IFN-γ receptors. The dependence of TLR on gp96 is not restricted to cell types, and the loss of gp96 cannot be compensated by any other chaperones in the ER, including calnexin, calreticulin (CRT), GRP78 (Bip), GRP170, ERp72, ERp57 (GRP58), and protein disulfide isomerase (PDI). By IB analysis, many of these chaperones showed no compensatory increase in gp96 mutant cells (Figure S3).

## Molecular Chaperoning of TLR9 by gp96

We next studied the mechanism by which gp96 regulates TLRs. Consistent with the established roles of gp96 in folding and cell-surface expression of TLRs (Randow and Seed, 2001), we found little surface expression of TLR2 and TLR4 on KO pMϕ (Figure 4A). In comparison, there was no reduction of cell-surface TLR2 and TLR4 on neutrophils from LysMcre$^{+/-}$*Hsp90b1*$^{flox/-}$ mice (Figure S4). To determine whether the failure of signaling via intracellular TLR in gp96-deficient cells was also due to the loss of chaperone function of gp96, we performed a series of studies focusing on TLR9. By a quantitative RT-PCR (Q-PCR), we found a similar amount of transcripts for TLR9, as well as for TLR2 and TLR4, in

WT and KO BMDM (Figure 4B). The expression of TLR9 protein by gp96-deficient Mϕ and B cells was abundant, as shown by IB with TLR9 Ab (Figure 4C). This experiment ruled out the possibility of problems with transcription and translation of TLR9 in gp96 KO cells; rather, the defect of TLR9 in the absence of gp96 was posttranslational.

HSPs are known to physically interact with their substrate proteins to facilitate folding. To determine whether gp96 interacts with TLR9, we expressed a tagged TLR9 in WT, KO BMDM, and HEK293 cells. The TLR9 was tagged at the C terminus with an epitope from the hemagglutinin (HA) of the influenza virus, which does not affect its function or intracellular distribution (Barton et al., 2006; Latz et al., 2004). As predicted, TLR9 was primarily distributed in the ER compartment and colocalized with gp96 by confocal analysis in WT BMDM (Figure 4D) and HEK293 cells (Figure 4E). The ER staining pattern of TLR9 was unaltered in the KO cells (Figure 4D). To demonstrate the direct interaction between the two proteins, we further immunoprecipited (IP) TLR9, followed by IB for gp96. gp96 could be coprecipitated with TLR9 only in TLR9 transfectants (Figure 4F) but not in HEK293 cells transfected with empty vector (data not shown). Interestingly, two forms of gp96 were coprecipitated with TLR9: a 96 kDa protein and a 110 kDa species that was due to hyperglycosylation of gp96 as indicated by the fact that the 110 kDa protein was converted to 96 kDa species by PNGase F and Endo H (Figure 4F). The sensitivity to Endo H supports the idea that the gp96-TLR9 interaction took place in the ER. Notably, 110 kDa superglycosylated gp96 was the minor species (less than 5%) in the cell, estimated by IB of total cell lysate (Figure 4G), which suggests that TLR9 preferentially interact with heavily glycosylated gp96. We also performed reciprocal IP with gp96 Ab followed by IB for TLR9. We found that SPA851, a rabbit polyclonal Ab against the C terminus of gp96 (aa 787–802), was able to co-IP both HA-tagged TLR9 in HEK293-TLR9 cells and the endogenous untagged TLR9 in BMDMs; 9G10, a rat monoclonal Ab (mAb) against gp96 280–344, was not able to co-IP TLR9 (Figure 4H). This experiment further confirmed the interaction between gp96 and TLR9; it suggests that 9G10 epitope is not accessible to 9G10 in gp96-TLR9 complexes, which is in line with the conformational disappearance of this epitope when gp96 is occupied by substrates such as radicicol (Loo et al., 1998; Vogen et al., 2002). Both free and complexed gp96 have the SPA851 epitope exposed because the C terminus of gp96 is not involved in the substrate binding (Argon and Simen, 1999; Yang and Li, 2005).

The mechanisms by which gp96 interacts and folds TLR9 were probed further with a number of pharmacological agents. Gp96 is an ER lectin, a $Ca^{2+}$ binding protein, as well as an ATP-binding molecule (Yang and Li, 2005). Any of these activities could be important for the TLR9-folding activity of gp96. To address this possibility, HEK293-TLR9 was treated with tunicamycin, an inhibitor of N-glycosylation; thapsigargin, an inhibitor of ER ATP-dependent $Ca^{2+}$ pump that causes depletion of ER calcium stores; and antimycin A, which depletes intracellular ATP pool. Cells were then lysed and TLR9 was immunoprecipited. We found that no gp96 was coprecipitated with TLR9 in the absence of N-linked glycosylation or when ER $Ca^{2+}$ store was depleted (Figure 4I). Lack of co-IP between gp96 and TLR9 in these conditions was not due to the absence of either protein, as indicated by the fact that IB of the whole-cell lysate revealed the abundance of both gp96 and TLR9. Depletion of ATP pool led to increased binding of TLR9 to unglycosylated gp96 in this assay.

In parallel, we also determined the binding characteristics between gp96 and TLR4 by using HEK293-TLR4 transfectants (Figure S5). We found both differences and similarities between TRL4 and TLR9. Both TLRs preferentially bound to glycosylated gp96, and the interaction was significantly inhibited by tunicamycin. However, the requirement for

calcium was more pronounced for TLR9-gp96 interaction in comparison to TLR4-gp96 interaction.

### Attenuation of Endotoxin Shock in Macrophage-Selective gp96-Deficient Mice

We have demonstrated that there was a general abrogation of TLR responsiveness in the Mϕ of LysMcre$^{+/-}$*Hsp90b1*$^{flox/-}$ mice, resulting from loss of the gp96 chaperone function. The categorical loss of TLR in Mϕ operationally created a mouse with multiple TLR defects. We then examined the importance of TLR-dependent function of Mϕ in inflammation and sepsis. Death from gram-negative bacteremia was primarily caused by vascular collapse, disseminated intravascular coagulation, and ischemic damage of vital organs as a result of systemic stimulation by endotoxin. TNF-α is the major mediator of such an endotoxemia (Beutler et al., 1985). Because TLR4 is expressed widely on B cells, neutrophils, DCs, Mϕ, as well as nonhematopoietic systems, it was unclear which cell type is the predominant source of TNF-α in sepsis. We challenged KO mice with LPS to address the roles of terminally differentiated Mϕ. 7-week-old WT and KO mice were administered i.p. with 0.5 mg LPS. Mice were bled at 0 (before LPS injection), 1.5, 3, and 6 hr after LPS injection. Serum IL-12p40, TNF-α, and IL-6 were quantified. We found that WT mice produced significantly more cytokines than did KO mice (Figures 5A and 5B). Consistent with the detrimental effect of these cytokines in sepsis, we found that the WT mice were more susceptible to LPS-induced sepsis than the KO mice. By day 4, 63% WT mice succumbed to endotoxemia. In contrast, 83% of KO mice survived to the same dose of LPS challenge (Figure 5C).

In the preceding experiment, LPS was administered i.p., which could be concentrated in the peritoneal cavity, resulting in preferential stimulation of pMϕ. To maximize LPS exposure to a variety of cell types including neutrophils, DC, and monocytes, in addition to Mϕ, we then injected LPS i.v. to both WT and KO mice. The KO mice were again more resistant to the LPS challenge than were WT mice, manifested by significantly reduced serum TNF-α (Figure 5D) and IL-12p40 (Figure 5E). Because the defect in TLR4 signaling is more pronounced in terminally differentiated Mϕ in KO mice, we conclude that tissue-derived Mϕ is the dominant source of proinflammatory cytokines in vivo during endotoxemia.

### High Susceptibility of LysMcre*Hsp90b1*$^{flox/-}$ Mice to *Listeria monocytogenes*

We next examined the function of gp96 null Mϕ in the clearance of *LM*, a gram-positive organism with abundant TLR ligands (Pamer, 2004). We challenged 7-week-old female KO mice and their littermates i.p. with $2 \times 10^6$ live *LmOVA*, a recombinant *LM* encoding a secreted form of chicken ovalbumin under the control of *hly* promoter (Pope et al., 2001). At 3 days after infections, significant weight loss was observed with KO mice (Figure 6A), accompanied by reduction of serum IL-12p40 (Figure 6B). Additionally, there was much more *LM* burden in the liver and the spleen of KO mice (Figure 6C). By histological analysis, the KO mice underwent total destruction of 60%–90% white pulp follicles in the spleen, with almost complete disappearance of lymphocytes (Figure 6D), whereas WT mice suffered only from moderate lymphocyte depletion, affecting <15% of follicles (Figure 6D). Livers of WT mice appeared grossly normal and showed no evidence of inflammation. There were numerous foci of necrosis and abscess in the livers of KO mice. Thus, Mϕ-specific ablation of gp96 confers high susceptibility to the infection by intracellular bacteria.

## DISCUSSION

TLRs have emerged as the critical sensors for recognition of PAMPs in microorganisms (Akira and Takeda, 2004; Medzhitov, 2001). Recognition of PAMPs sets up a series of motions aimed to eradicate these pathogens and to ensure the survival of the host, including

unleashing the direct bactericidal functions of the mononuclear phagocyte system (Laroux et al., 2005), producing proinflammatory cytokines, and ramping up the host defenses by efficiently priming the adaptive immune response. Therefore, understanding the regulation of the TLR system is fundamentally important in designing therapeutic strategies against both the existing and emerging infectious agents. Great progress has been made in discerning the TLR-signaling pathways (Akira and Takeda, 2004). However, less attention has been paid to the regulation of the expression of TLRs for understanding the mechanism of TLR downregulation in inflammation (Nomura et al., 2000), the basis for cell- and tissue-specific distribution of TLRs (Iwasaki and Medzhitov, 2004), and the linkage of TLR inducibility to both physiological and pathological conditions (Liu et al., 2006).

In this study, we have revealed that both intracellular and cell-surface TLRs are functionally dependent on an ER chaperone gp96. By conditionally ablating gp96 genetically, we found that the normal level of gp96 is not required for the differentiation, survival, or cytokine-mediated activation of Mϕ. However, gp96-deficient Mϕ failed to respond to ligands for TLR2, TLR4, TLR5, TLR7, and TLR9. We have also demonstrated that gp96 binds directly to TLR9 and TLR4; the loss of TLR function in gp96 null cells was not due to transcriptional or translational defect. These data, coupled with the seminal finding that gp96 chaperones TLR1, TLR2, and TLR4 (Randow and Seed, 2001), demonstrate that gp96 is the master immune chaperone for TLRs.

We found that gp96 interacts with TLR9 in a manner that is dependent on ER $Ca^{2+}$ store and N-linked glycosylation, indicating that the interaction between the two proteins is an active process, not a result of nonspecific passive interaction. Similarly, TLR4 also requires $Ca^{2+}$ store, albeit to a lesser degree, for interaction with gp96. Interestingly, the hyperglycosylated gp96 species normally accounts for only ~5% of the total gp96 in the cells, and yet >50% of gp96 in the complexes with either TLR4 or TLR9 were hyperglycosylated. Such a preferential binding of the hyperglycosylated gp96 to TLR suggests that this interaction is cotranslational and occurs transiently before N-linked glycan of gp96 is trimmed in the ER. This transient interaction most likely reflects the rapid folding of TLR. Similar to other client proteins of gp96 (Kuznetsov et al., 1996; Vandenbroeck et al., 2006), when the intracellular ATP store is depleted, the complex formation between TLR and gp96 increases markedly, indicating that the dissociation between gp96 and TLRs is probably dependent on ATP binding and ATP hydrolysis, both of which have been found to be critical for the TLR chaperone function of gp96 (Randow and Seed, 2001). Further studies are necessary to determine whether ATP, $Ca^{2+}$, and glycosylation exert their effects on TLR-gp96 interaction directly or indirectly.

Our results are important for several reasons. First, there are numerous HSPs in the ER that can potentially chaperone TLRs, including calnexin, grp78, calreticulin, protein disulfide isomerase, and thiol-oxidoreductase ERp57. Many of these proteins form a superchaperone complex to assist client protein folding (Meunier et al., 2002; Vandenbroeck et al., 2006). Our results demonstrate that the function of gp96 in folding TLRs cannot be replaced by any other chaperones. Indeed, by IB, we did not observe any compensatory increase of other HSPs in gp96 null cells. Second, the immune chaperone function of gp96 is not restricted to TLR1, TLR2, TLR5, and TLR4, but also encompasses intracellular TLRs including TLR7 and TLR9. This finding suggests that there is a common pathway for TLR protein maturation that is critically dependent on gp96. In this regard, gp96 clearly plays a different role from 3d, another ER resident protein that is essential for the function of TLR3, 7, and 9, but not for TLR1, 2, and 4 (Tabeta et al., 2006). Third, our study is the first to probe the function of the HSP90 family on the biology of Mϕ genetically. Surprisingly, other than the loss of response to innate immune stimuli, the development and function of Mϕ are preserved in the absence of gp96.

gp96 KO mice produced significantly less IL-12p40 and TNF-α in response to both systemic LPS and *Listeria*, even though the only defect in these mice appeared to be tissue-resident Mϕ. Our study clearly implicated Mϕ but not DCs as the dominant source of proinflammatory cytokines during endotoxemia and *Listeria* infection. In the case of *Listeria* infection, the reduced IL-12p40 production could not be attributed to reduced stimuli, because there was more bacteria burden in infected KO mice. gp96 has been suggested to be a receptor for a virulence factor of *Listeria*, Vip, on some epithelial cells (Cabanes et al., 2005). However, the same study reveals no roles of gp96-Vip interaction for *LM* entry into Mϕ: Mϕ does not express gp96 on cell surface. The increased susceptibility of gp96 KO mice is thus more consistent with the essential roles of both TLR and Mϕ in the acute host defense against *Listeria* (Pamer, 2004).

There are at least four receptors that are critical for sensing dsRNA in mice: these receptors are TLR3, dsRNA-dependent protein kinase PKR, Mda-5, and Rig-I (Gitlin et al., 2006; Ishii et al., 2006; Kato et al., 2005). For unknown reasons, the dominance of these receptors is dependent on cell types as well as the strains of RNA virus. Whereas type I IFN production by DCs is almost exclusively dependent on Mda-5, production of proinflammatory cytokines by pMϕ in response to poly I:C is mainly mediated by TLR3-Trif pathway (Gitlin et al., 2006). TNF-α production was reduced from gp96-deficient pMϕ in response to poly I:C, arguing that gp96 is also important for TLR3 function. However, to what extent gp96 contributes to TLR3 function awaits future functional as well as biochemical studies with multiple gp96-deficient cell types in response to a variety of RNA virus besides poly I:C. Similarly, further studies are required to prove our hypothesis that gp96 is also a molecular chaperone for TLR11, because experiments with the profilin-like protein *T. gondii* (Yarovinsky et al., 2005) were inconclusive (data not shown), perhaps because of a low level of TLR11 expression in Mϕ.

In summary, our study represents an effort to address the immunological roles of gp96 on the biology of Mϕ in vivo. Our results demonstrate that gp96 is the master immune chaperone for both cell-surface and intracellular TLRs including TLR1, 2, 4, 5, 7, and 9, and that Mϕ are the dominant source of proinflammatory cytokines during endotoxemia and *Listeria* infection. The loss of most TLR functions by gp96-deficient Mϕ operationally created a Mϕ-selective global TLR-deficient mouse. This model should be useful for addressing the roles of gp96 in immune responses in general and for discerning the TLR-dependent functions of Mϕ in the broad context of infection, inflammation, cancer, and autoimmune diseases.

## EXPERIMENTAL PROCEDURES

### Mice

Gp96 conditional deficient mice were generated by homologous recombination. In brief, a 17 kb mouse genomic DNA fragment was cloned from the mouse 129Sv/Ev lambda genomic library. This genomic fragment contained exon 1–4 of *Hsp90b1*. The targeting vector was constructed to insert the Neo gene cassette (flanked by loxP sites) before the exon 1 (containing ATG). The third loxP site was inserted 230 bp downstream of exon 1. A HSV-tk cassette was introduced at the 3′ end of the genomic fragment (Figure 1A).

10 μg of the targeting vector was linearized by NotI and then transfected by electroporation of 129/SvEv embryonic stem (ES) cells. After double selection in G418 and gancyclovir, 250 surviving colonies were expanded for PCR analysis to identify recombinant clones. The correctly targeted ES cell line was microinjected into the C57BL/6J blastocysts and produced four female chimeras (100% agouti). The chimeric mice were then mated to generate germline transmission of the *Hsp90b1*$^{flox}$ mice as described in the Results.

LysMcre mice were purchased from Jackson Laboratories (Bar Harbor, ME). EIIa-cre mice and Z/EG mice were provided by C. Guo (University of Connecticut, Farmington, CT). The *Tlr2*$^{-/-}$-*Tlr4*$^{-/-}$ mice were generated by intercrossing *Tlr2*$^{-/-}$ and *Tlr4*$^{-/-}$ mice, which were obtained from R. Medzhitov (Yale University, New Haven, CT). Animal use was approved by the University of Connecticut Health Center Animal Care Committee.

### Reagents

LPS (from *Escherichia coli*, serotype O55:B5) was obtained from Sigma (St. Louis, MO). All other TLR ligands were purchased from InvivoGen (San Diego, CA). Recombinant murine IL-1β and IFN-γ and TNF-α were obtained from Endogen (Rockford, IL) and BD Pharmingen (San Diego, CA), respectively.

### Antibodies

All Abs were obtained from *e*Bioscience (San Diego, CA), except PDCA-1 Ab (Miltenyi, Auburn, CA), gp96 Abs (9G10 and SPA-851) (Stressgen, Victoria, BC, Canada), and β-actin Ab (AC-74, Sigma).

### Culture of Bone Marrow-Derived Macrophages

Bone marrow cells were isolated and cultured in Mϕ growth medium (DMEM supplemented with 10% FCS, 100 U/ml of penicillin, 100 μg/ml of streptomycin, 2 mM L-glutamine, 20% L929 condition medium) for 6 days. Nonadherent cells were washed away, and adherent cells were harvested after trypsin digestion. This method consistently gave rise to more than 98% F4/80$^{+}$ cells by flow cytometry (data not shown).

### Flow Cytometry

Surface staining of cells and flow cytometry were done as described (Liu et al., 2003; Zheng and Li, 2004). To stain gp96 intracellularly, cells were fixed in 4% paraformaldehyde and permeablized in ice-cold methanol. To stain mouse cytokines, cells were fixed in the same way but permeablized with 0.25% saponin. Cells were acquired on Calibur (Becton Dickinson, Franklin Lakes, NJ) and results were analyzed with FloJo software (Tree Star, Ashland, OR).

### Cell Lines and Immunoprecipitation

HEK293 cells were obtained from ATCC (Manassas, VA) and transfected transiently with either TLR9-HA or TLR4-HA expression vector (pUNO-TLR-HA, InvivoGen, San Diego, CA) via lipofectamine (Invitrogen, Carlsbad, CA). 30 hr later, cells were treated with medium only, tunicamycin, antimycin A, or thapsigargin (Sigma) for 18 hr. Cells were then lysed in the presence of RIPA lysis buffer (0.01 M sodium phosphate [pH 7.2], 150 mM NaCl, 2 mM EDTA, 1% NP-40, 1% sodium deoxycholate, 0.1% SDS, 2 mM AEBSF, 130 μM bestatin, 14 μM E-64, 0.3 μM aprotinin, and 1 mM leupeptin), followed by centrifugation to remove nuclei. The supernatants were then incubated with Ab and 40 μl of protein A/G-Sepharose beads (Sigma) for 16 hr at 4°C, followed by extensive washing in the cold lysis buffer and elution of immunoprecipitates by boiling protein A/G beads in the SDS-PAGE sample buffer. In some experiments, the immunoprecipitates were eluted and digested with Endo Hf or PNGase F according to the manufacturer's protocol (New England BioLab, Ipswich, MA). The samples were resolved by 8%–10% denaturing and reducing SDS-PAGE, and they were analyzed by IB with HRP-based secondary Ab with either high-sensitive or low-sensitive substrates that were converted to chemiluminescent products (Pierce, Rockford, IL).

### Retroviral Transduction and Confocal Microscopy

2 days before staining for confocal analysis, HEK293 cells were transiently transfected with pUNO-TLR9-HA as described above. BMDMs were transduced with a retroviral vector expressing TLR9-HA and enhanced GFP (EGFP) in the bicistronic fashion. In brief, TLR9-HA from pUNO-TLR9-HA was amplified by polymerase chain reaction and subcloned into the BglII site on MigR1 retrovector. Ecotropic TLR9-HA retroviruses were packaged in the Pheonix-Ecotropic cell line. For confocal analysis, cells were seeded and cultured on glass coverslips at 37°C overnight, washed with 1× PBS, fixed immediately with 2% paraformaldehyde, permeablized with 100% cold methanol, and blocked for 30 min in 5% normal goat serum. Cells were double stained for 1 hr at room temperature with gp96 Ab 9G10 and HA mAb (Covance, Princeton, NJ). After extensive washing, all samples were incubated with polyclonal goat anti-mouse Alexa Fluor 647 (TLR9, red) and polyclonal goat anti-rat Alexa Fluor 488/Rhodomine Red (gp96, green) secondary Ab. Nuclei were counterstained with propidium iodide (PI). Single stainings with primary and secondary Ab alone were also performed to ensure specificity (data not shown). Samples were mounted onto glass slides with a mounting medium (Biomedia, Foster City, CA) to retard photobleaching, sealed with nail enamel, and imaged with a Zeiss LSM 510 Axiovert 100 confocal microscope equipped with an argon/krypton laser (Zeiss, Chester, VA).

### Quantitative RT-PCR

Day 6 BMDM were harvested. Total RNA was extracted with the NucleoSpin RNA II kit according to the manufacturer's protocol (Clontech, Mountain View, CA). The mRNA was reverse transcribed with Superscript II (Invitrogen, Carlsbad, CA). cDNA was quantified by Q-PCR with Bio-Rad iCycler. Q-PCR data were analyzed with the corresponding software, and the number of PCR cycles to reach the threshold of detection (CT) was calculated. Samples were run in duplicates. Hypoxanthine-guanine phosphoribosyl transferase (HPRT) was used as an internal control. The primer sequences are as follows. mTLR2F, CAGACGTAGTGAGCGAGCTG; mTLR2R, GGCATCGGATGAAAAGTGTT; mTLR4F, GCTTTCACCTCTGCCTTCAC; mTLR4R, CGAGGCTTTTCCATCCAATA; mTLR9F, ACCCTGGTGTGGAACATCAT; mTLR9R, GTTGGACAGGTGGACGAAGT; HPRT-F, GCCGACCCGCAGTCCCAGC; HPRT-R, TTAGGCTTTGTATTTGGCTTTTC.

### LPS Challenging

Sex- and age-matched mice were injected i.p. with 0.5 mg LPS or i.v. with 1 mg LPS per mouse. Serum was obtained at different time points post injection. Mice were then followed clinically.

### *Listeria* Infection

Sex- and age-matched mice were inoculated with $2 \times 10^6$ *LM* intraperitoneally. Serum was obtained every 24 hr after infection. At day 3, mice were sacrificed; spleens and livers were harvested, dissociated, and homogenized in 1% saponin/PBS. Bacteria CFUs were determined by plating serial dilutions of the homogenate on brain-heart infusion agar plates and incubating at 37°C overnight. Parts of organs were fixed in 10% formalin, sectioned, and processed for hematoxylin and eosin staining according to standard protocols.

### ELISA

IL-12p40, IL-6, and TNF-α levels in the serum and culture supernatant were measured with ELISA kits from BD Biosciences (San Diego, CA) according to the manufacturer's protocol.

### Nitrite Assay

Nitrite in supernatants was measured with the Griess Reagent Kit (Molecular Probes, Eugene, OR) with $NaNO_2$ as the standard.

## Supplementary Material

Refer to Web version on PubMed Central for supplementary material.

## Acknowledgments

We thank C. Guo, J. Li, A. Lichtler, A. Vella, A. Adler, L. Aguila, D. Wu, and B. Seed for providing valuable reagents and expertise; T. Siddiqi for the initial Southern blot analysis of *Hsp90b1*$^{flox}$ mice; M. Caudill for HSP profiling in gp96 mutant pre-B cells; M. Staron for sharing some unpublished data; and students and faculty members in the Immunology Graduate Program for helpful discussions. This work was supported in part by the National Institutes of Health grants CA100191 (Z.L.) and P01-AI56172 (L.L.).

## REFERENCES

Akira S, Takeda K. Toll-like receptor signalling. Nat. Rev. Immunol 2004;4:499–511. [PubMed: 15229469]

Argon Y, Simen BB. GRP94, an ER chaperone with protein and peptide binding properties. Semin. Cell Dev. Biol 1999;10:495–505. [PubMed: 10597632]

Barton GM, Kagan JC, Medzhitov R. Intracellular localization of Toll-like receptor 9 prevents recognition of self DNA but facilitates access to viral DNA. Nat. Immunol 2006;7:49–56. [PubMed: 16341217]

Bettelli E, Carrier Y, Gao W, Korn T, Strom TB, Oukka M, Weiner HL, Kuchroo VK. Reciprocal developmental pathways for the generation of pathogenic effector TH17 and regulatory T cells. Nature 2006;441:235–238. [PubMed: 16648838]

Beutler B, Milsark IW, Cerami AC. Passive immunization against cachectin/tumor necrosis factor protects mice from lethal effect of endotoxin. Science 1985;229:869–871. [PubMed: 3895437]

Cabanes D, Sousa S, Cebria A, Lecuit M, Garcia-del Portillo F, Cossart P. Gp96 is a receptor for a novel *Listeria monocytogenes* virulence factor, Vip, a surface protein. EMBO J 2005;24:2827–2838. [PubMed: 16015374]

Chuang TH, Ulevitch RJ. Triad3A, an E3 ubiquitin-protein ligase regulating Toll-like receptors. Nat. Immunol 2004;5:495–502. [PubMed: 15107846]

Clausen BE, Burkhardt C, Reith W, Renkawitz R, Forster I. Conditional gene targeting in macrophages and granulocytes using LysMcre mice. Transgenic Res 1999;8:265–277. [PubMed: 10621974]

Gitlin L, Barchet W, Gilfillan S, Cella M, Beutler B, Flavell RA, Diamond MS, Colonna M. Essential role of mda-5 in type I IFN responses to polyriboinosinic:polyribocytidylic acid and encephalomyocarditis picornavirus. Proc. Natl. Acad. Sci. USA 2006;103:8459–8464. [PubMed: 16714379]

Hawn TR, Wu H, Grossman JM, Hahn BH, Tsao BP, Aderem A. A stop codon polymorphism of Toll-like receptor 5 is associated with resistance to systemic lupus erythematosus. Proc. Natl. Acad. Sci. USA 2005;102:10593–10597. [PubMed: 16027372]

Ishii KJ, Coban C, Kato H, Takahashi K, Torii Y, Takeshita F, Ludwig H, Sutter G, Suzuki K, Hemmi H, et al. A Toll-like receptor-independent antiviral response induced by double-stranded B-form DNA. Nat. Immunol 2006;7:40–48. [PubMed: 16286919]

Iwasaki A, Medzhitov R. Toll-like receptor control of the adaptive immune responses. Nat. Immunol 2004;5:987–995. [PubMed: 15454922]

Kato H, Sato S, Yoneyama M, Yamamoto M, Uematsu S, Matsui K, Tsujimura T, Takeda K, Fujita T, Takeuchi O, Akira S. Cell type-specific involvement of RIG-I in antiviral response. Immunity 2005;23:19–28. [PubMed: 16039576]

Kozutsumi Y, Segal M, Normington K, Gething MJ, Sambrook J. The presence of malfolded proteins in the endoplasmic reticulum signals the induction of glucose-regulated proteins. Nature 1988;332:462–464. [PubMed: 3352747]

Kuznetsov G, Bush KT, Zhang PL, Nigam SK. Perturbations in maturation of secretory proteins and their association with endoplasmic reticulum chaperones in a cell culture model for epithelial ischemia. Proc. Natl. Acad. Sci. USA 1996;93:8584–8589. [PubMed: 8710914]

Lakso M, Pichel JG, Gorman JR, Sauer B, Okamoto Y, Lee E, Alt FW, Westphal H. Efficient in vivo manipulation of mouse genomic sequences at the zygote stage. Proc. Natl. Acad. Sci. USA 1996;93:5860–5865. [PubMed: 8650183]

Laroux FS, Romero X, Wetzler L, Engel P, Terhorst C. Cutting edge: MyD88 controls phagocyte NADPH oxidase function and killing of gram-negative bacteria. J. Immunol 2005;175:5596–5600. [PubMed: 16237045]

Latz E, Schoenemeyer A, Visintin A, Fitzgerald KA, Monks BG, Knetter CF, Lien E, Nilsen NJ, Espevik T, Golenbock DT. TLR9 signals after translocating from the ER to CpG DNA in the lysosome. Nat. Immunol 2004;5:190–198. [PubMed: 14716310]

Lee AS, Delegeane A, Scharff D. Highly conserved glucose-regulated protein in hamster and chicken cells: preliminary characterization of its cDNA clone. Proc. Natl. Acad. Sci. USA 1981;78:4922–4925. [PubMed: 6946438]

Li Z, Srivastava PK. Tumor rejection antigen gp96/grp94 is an ATPase: implications for protein folding and antigen presentation. EMBO J 1993;12:3143–3151. [PubMed: 8344253]

Liew FY, Xu D, Brint EK, O'Neill LA. Negative regulation of toll-like receptor-mediated immune responses. Nat. Rev. Immunol 2005;5:446–458. [PubMed: 15928677]

Liu B, Dai J, Zheng H, Stoilova D, Sun S, Li Z. Cell surface expression of an endoplasmic reticulum resident heat shock protein gp96 triggers MyD88-dependent systemic autoimmune diseases. Proc. Natl. Acad. Sci. USA 2003;100:15824–15829. [PubMed: 14668429]

Liu B, Yang Y, Dai J, Medzhitov R, Freudenberg MA, Zhang PL, Li Z. TLR4 up-regulation at protein or gene level is pathogenic for lupus-like autoimmune disease. J. Immunol 2006;177:6880–6888. [PubMed: 17082602]

Loo MA, Jensen TJ, Cui L, Hou Y, Chang XB, Riordan JR. Perturbation of Hsp90 interaction with nascent CFTR prevents its maturation and accelerates its degradation by the proteasome. EMBO J 1998;17:6879–6887. [PubMed: 9843494]

Medzhitov R. Toll-like receptors and innate immunity. Nat. Rev. Immunol 2001;1:135–145. [PubMed: 11905821]

Melnick J, Dul JL, Argon Y. Sequential interaction of the chaperones BiP and GRP94 with immunoglobulin chains in the endoplasmic reticulum. Nature 1994;370:373–375. [PubMed: 7913987]

Meunier L, Usherwood YK, Chung KT, Hendershot LM. A subset of chaperones and folding enzymes form multiprotein complexes in endoplasmic reticulum to bind nascent proteins. Mol. Biol. Cell 2002;13:4456–4469. [PubMed: 12475965]

Nishiya T, Kajita E, Miwa S, Defranco AL. TLR3 and TLR7 are targeted to the same intracellular compartments by distinct regulatory elements. J. Biol. Chem 2005;280:37107–37117. [PubMed: 16105838]

Nomura F, Akashi S, Sakao Y, Sato S, Kawai T, Matsumoto M, Nakanishi K, Kimoto M, Miyake K, Takeda K, Akira S. Cutting edge: endotoxin tolerance in mouse peritoneal macrophages correlates with down-regulation of surface toll-like receptor 4 expression. J. Immunol 2000;164:3476–3479. [PubMed: 10725699]

Novak A, Guo C, Yang W, Nagy A, Lobe CG. Z/EG, a double reporter mouse line that expresses enhanced green fluores-cent protein upon Cre-mediated excision. Genesis 2000;28:147–155. [PubMed: 11105057]

O'Neill LA, Fitzgerald KA, Bowie AG. The Toll-IL-1 receptor adaptor family grows to five members. Trends Immunol 2003;24:286–290. [PubMed: 12810098]

Pamer EG. Immune responses to *Listeria monocytogenes*. Nat. Rev. Immunol 2004;4:812–823. [PubMed: 15459672]

Pasare C, Medzhitov R. Toll pathway-dependent blockade of CD4+CD25+ T cell-mediated suppression by dendritic cells. Science 2003;299:1033–1036. [PubMed: 12532024]

Pasare C, Medzhitov R. Toll-dependent control mechanisms of CD4 T cell activation. Immunity 2004;21:733–741. [PubMed: 15539158]

Pope C, Kim SK, Marzo A, Masopust D, Williams K, Jiang J, Shen H, Lefrancois L. Organ-specific regulation of the CD8 T cell response to *Listeria monocytogenes* infection. J. Immunol 2001;166:3402–3409. [PubMed: 11207297]

Randow F, Seed B. Endoplasmic reticulum chaperone gp96 is required for innate immunity but not cell viability. Nat. Cell Biol 2001;3:891–896. [PubMed: 11584270]

Roach JC, Glusman G, Rowen L, Kaur A, Purcell MK, Smith KD, Hood LE, Aderem A. The evolution of vertebrate Toll-like receptors. Proc. Natl. Acad. Sci. USA 2005;102:9577–9582. [PubMed: 15976025]

Schnare M, Barton GM, Holt AC, Takeda K, Akira S, Medzhitov R. Toll-like receptors control activation of adaptive immune responses. Nat. Immunol 2001;2:947–950. [PubMed: 11547333]

Shortman K, Liu YJ. Mouse and human dendritic cell subtypes. Nat. Rev. Immunol 2002;2:151–161. [PubMed: 11913066]

Srivastava PK, DeLeo AB, Old LJ. Tumor rejection antigens of chemically induced sarcomas of inbred mice. Proc. Natl. Acad. Sci. USA 1986;83:3407–3411. [PubMed: 3458189]

Stoilova D, Dai J, de Crom R, van Haperen R, Li Z. Haplosufficiency or functional redundancy of a heat shock protein gp96 gene in the adaptive immune response. Cell Stress Chaperones 2000;5:395.

Tabeta K, Hoebe K, Janssen EM, Du X, Georgel P, Crozat K, Mudd S, Mann N, Sovath S, Goode J, et al. The Unc93b1 mutation 3d disrupts exogenous antigen presentation and signaling via Toll-like receptors 3, 7 and 9. Nat. Immunol 2006;7:156–164. [PubMed: 16415873]

Takeda K, Akira S. Toll-like receptors in innate immunity. Int. Immunol 2005;17:1–14. [PubMed: 15585605]

Vandenbroeck K, Martens E, Alloza I. Multi-chaperone complexes regulate the folding of interferon-gamma in the endoplasmic reticulum. Cytokine 2006;33:264–273. [PubMed: 16574426]

Vogen S, Gidalevitz T, Biswas C, Simen BB, Stein E, Gulmen F, Argon Y. Radicicol-sensitive peptide binding to the N-terminal portion of GRP94. J. Biol. Chem 2002;277:40742–40750. [PubMed: 12189140]

Wang T, Chuang TH, Ronni T, Gu S, Du YC, Cai H, Sun HQ, Yin HL, Chen X. Flightless I homolog negatively modulates the TLR pathway. J. Immunol 2006;176:1355–1362. [PubMed: 16424162]

Yang Y, Li Z. Roles of heat shock protein gp96 in the ER quality control: redundant or unique function? Mol. Cells 2005;20:173–182. [PubMed: 16267390]

Yarovinsky F, Zhang D, Andersen JF, Bannenberg GL, Serhan CN, Hayden MS, Hieny S, Sutterwala FS, Flavell RA, Ghosh S, Sher A. TLR11 activation of dendritic cells by a protozoan profilin-like protein. Science 2005;308:1626–1629. [PubMed: 15860593]

Ye M, Iwasaki H, Laiosa CV, Stadtfeld M, Xie H, Heck S, Clausen B, Akashi K, Graf T. Hematopoietic stem cells expressing the myeloid lysozyme gene retain long-term, multilineage repopulation potential. Immunity 2003;19:689–699. [PubMed: 14614856]

Zheng H, Li Z. Cutting edge: cross-presentation of cell-associated antigens to MHC class I molecule is regulated by a major transcription factor for heat shock proteins. J. Immunol 2004;173:5929–5933. [PubMed: 15528326]

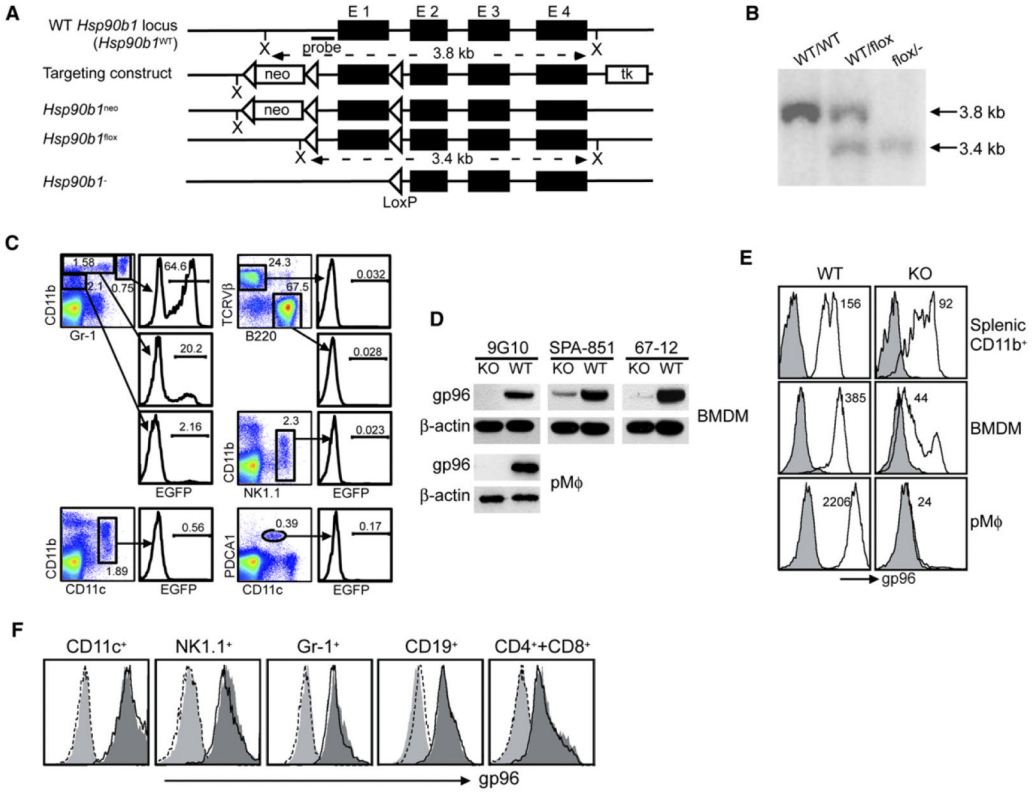


**Figure 1. Generation of a Conditional gp96-Deficient Mouse**

(A) The scheme of targeting *Hsp90b1* locus and expected sequence of *Hsp90b1* loci after cre-mediated recombination. Neo, neomycin phosophotransferase; tk, thymidine kinase; X, XbaI; E, exon.

(B) Confirmation of targeted *Hsp90b1* allele by Southern blot with probe indicated in (A).

(C) Flow cytometric analysis of GFP activity in various subsets of splenocytes of LysMcre$^{+}$ Z/EG mice. Percent of GFP$^{+}$ cells is indicated.

(D) IB analysis of gp96 in BMDM and pMϕ from LysMcre$^{+/-}$*Hsp90b1*$^{flox/-}$ and control mice.

(E) Quantification of gp96 in splenic CD11b$^{+}$ cells, BMDM, as well as pMf by intracellular staining (gp96, open histogram; isotype control, shaded histogram). Number represents the mean fluorescence intensity of gp96 stain.

(F) Intracellular analysis of gp96 in different lineages of hematopoietic cells in the spleens of KO (open histogram with solid line) and WT (dark gray-shaded histogram) mice. Histograms at the far left represent isotype controls that are superimposable between KO (open histogram with dotted line) and WT (light gray-shaded histogram) mice. More than three experiments were done with the similar results.

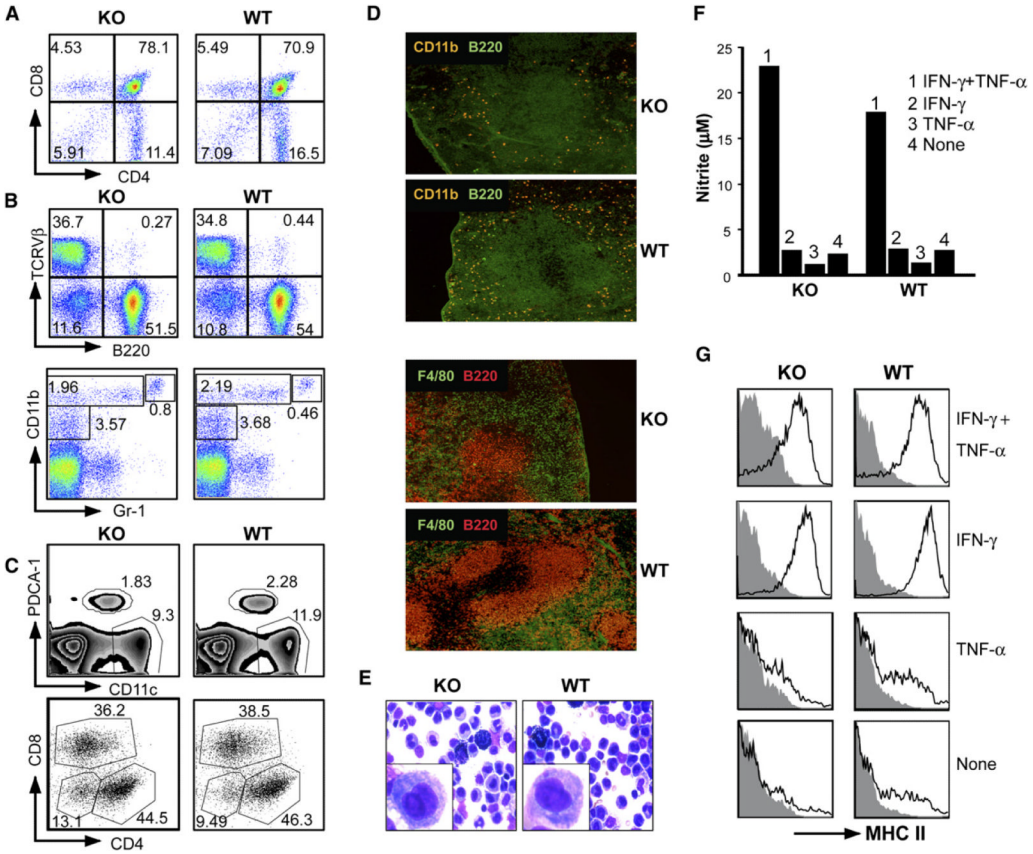


**Figure 2. Normal Hematopoiesis, Differentiation, and Cytokine-Mediated Activation of Mϕ in LysMcre$^{+/-}$*Hsp90b1*$^{flox/-}$ Mice**

(A) Thymocytes of KO or control littermates were stained for CD4 and CD8, followed by flow cytometric analysis.

(B) Analysis of splenocytes by flow cytometry. RBC-depleted and collagenase-treated single-cell suspensions of splenocytes were stained with a combination of either Ab against TCR Vβ and B220 or Ab against CD11b and Gr-1.

(C) Analysis of splenic DC based on expression of CD11c and a plasmacytoid DC marker, pDCA-1. CD11c$^{+}$ DC were then further analyzed for the expression of CD4 and CD8. Numbers represent percent of cells in each quadrant or the marked area over the total cellular populations.

(D) Immunofluorescence microscopy of WT or gp96 KO spleens. WT and gp96 KO mice were sacrificed. 5 mμ cryosections were prepared and stained with Ab against B220/CD11b and B220/F4/80, followed by immunofluorescence microscopy (×100).

(E) WT and KO PECs were harvested, plated on glass slides by cytospin, and stained with Hema-3 reagent. Inset is a magnification of one representative monocytic/Mϕ cell.

(F) F4/80$^{+}$ pMϕ were treated with TNF-α (10 ng/ml), IFN-γ (500 U/ml), or a combination of both for 16 hr, followed by the measurement of NO in the supernatant.

(G) Cells from (F) were analyzed by flow cytometry for cell-surface expression of I-A/E (MHC class II). Numerous experiments were done with the similar results.

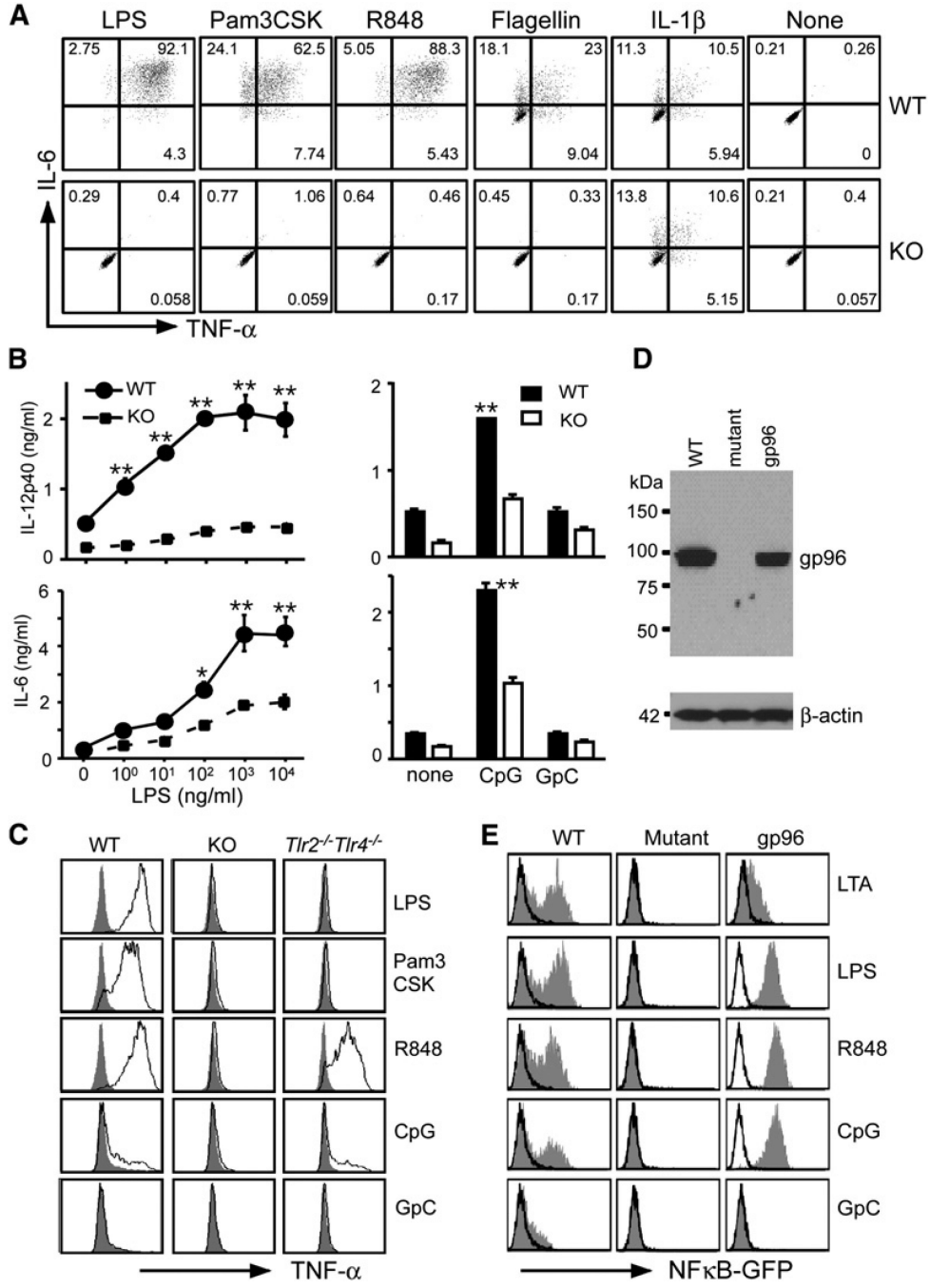


**Figure 3. Loss of Responsiveness of gp96 Null Cells to the Ligands of Both Intracellular and Cell-Surface TLRs**

(A) PECs of the KO and WT mice were treated with LPS (100 ng/ml), Pam3CSK4 (1 μg/ml), R848 (1 μg/ml), flagellin (100 ng/ml), or IL-1β (100 ng/ml), followed by intracellular stain for TNF-α and IL-6. F4/80$^+$ cells were gated on. At least five experiments were done with similar results.

(B) BMDMs were incubated with LPS at the indicated concentrations, CpG or control oligonucleotide (GpC) at 1 μM for 4 hr. Supernatant was harvested; IL-6 and IL-12p40 were measured by ELISA in triplicates (mean ± SEM). *$p < 0.05$; **$p < 0.01$. The data are representative of three independent experiments.

(C) Loss of TLR7 and TLR9 responses by gp96 KO Mϕ was not due to absence of TLR2 and TLR4. PEC cells were collected from WT, KO, and *Tlr2*$^{-/-}$*TLR4*$^{-/-}$ mice, stimulated with 100 ng/ml LPS, 1 μg/ml Pam3Cysk4, and 1 μg/ml R848 for 5 hr, followed by intracellular staining for TNF-α. F4/80$^{+}$ cells were gated on. For examining TLR9 responsiveness, PECs were primed with 500 U/ml IFN-γ for 20 hr, followed by stimulation with 1 μM CpG or GpC for another 5 hr. Shaded histograms represented staining for TNF-α without ligand stimulation. Two experiments were performed with the similar results.
(D) IB of gp96 in WT, mutant pre-B cell, as well as mutant cell transfected with a gp96 expression vector. β-actin was blotted to serve as a loading control. Numbers represent M.W. markers.
(E) Restoration of response of mutant pre-B cells to TLR ligands by stable expression of gp96. Various cells were stimulated with TLR ligands for 24 hr, followed by flow cytometry for GFP expression. Open and shaded histogram represents cells cultured in medium and stimulators, respectively. Numerous experiments were done with similar findings.

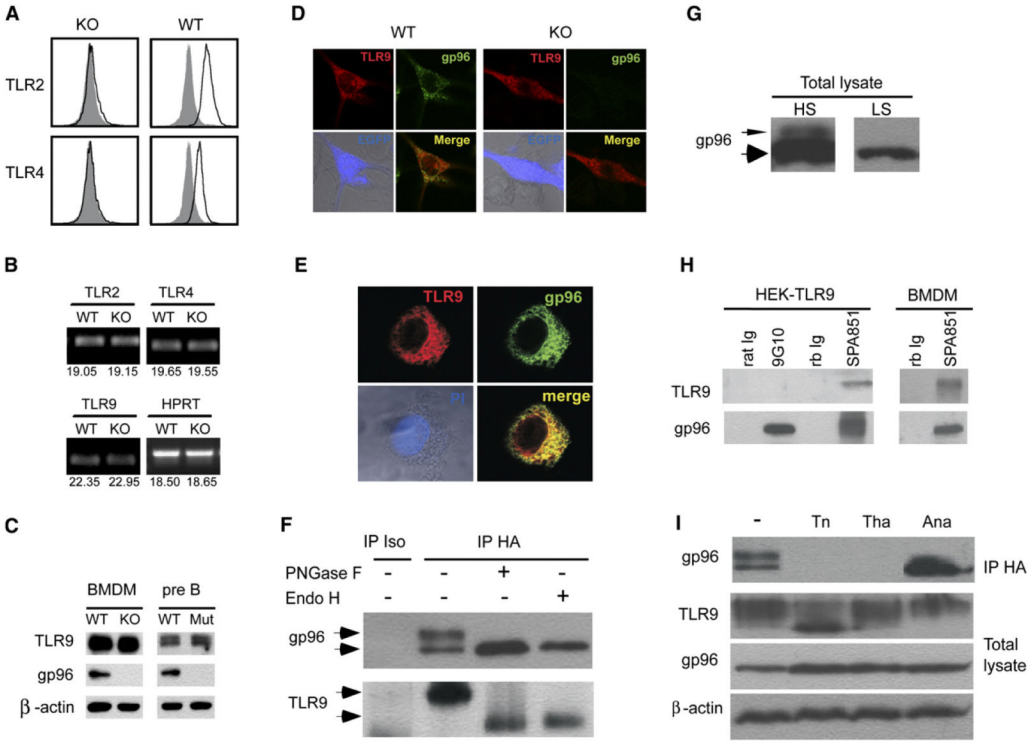


**Figure 4. gp96 Is a Molecular Chaperone for TLR9**

(A) The WT and gp96-deficient F4/80$^+$ cells were analyzed for cell-surface expression of TLR2 and TLR4 (open histogram). Shaded histogram represents isotype control.

(B) Comparative TLR mRNA level in WT and KO BMDM by Q-PCR. Number below represents number of threshold cycle (average of 2 duplicate runs).

(C) IB analysis of TLR9, gp96, and β-actin in WT and KO cells.

(D) Confocal analysis of TLR9 and gp96 expression in WT and KO BMDMs. Day +3 WT or KO BMDMs were transduced with a retroviral vector expressing TLR9-HA and enhanced GFP (EGFP) in the bicistronic fashion. 2 days later, cells were seeded and cultured on glass coverslips, fixed, permeablized, blocked, and double stained with mouse anti-HA Ab and rat anti-gp96 Ab, followed by goat anti-mouse Alexa Fluor 647 (TLR9, red) and goat anti-rat Alexa Fluor 488/Rhodomine Red (gp96, green) secondary Ab. Images were captured with a Zeiss LSM 510 Axiovert 100 confocal microscope equipped with an argon/krypton laser.

(E) Confocal analysis of TLR9 expression. HEK293-TLR9 cells were cultured on glass coverslips, fixed, permeablized, and stained for gp96 (green) and TLR9 (red). The nucleus was counterstained with PI (blue). The merged images (gp96 and TLR9, light transmission and PI) were also shown.

(F) gp96 is coprecipitated with TLR9. HEK293-TLR9 cells were immunoprecipitated with HA Ab or isotype control Ab, treated with nothing, PNGase F, or Endo H, followed by IB for gp96 and TLR9.

(G) Total cell lysates of HEK293-TLR9 were immunoblotted for gp96, developed with substrates of either high sensitivity (HS) or low sensitivity (LS).

(H) HEK293-TLR9 cells or WT BMDM were immunoprecipitated with 9G10, SPA851, or respective isotype control Ab, followed by SDA-PAGE and IB for gp96 and TLR9.

(I) HEK293-TLR9 cells were treated with buffer only, tunicamycin, thapsigargin, or antimycin A. Cells were then immunoprecipitated for TLR9 followed by IB for gp96; the aliquot of the total cell lysates were immunoblotted for gp96, TLR9, and β-actin.

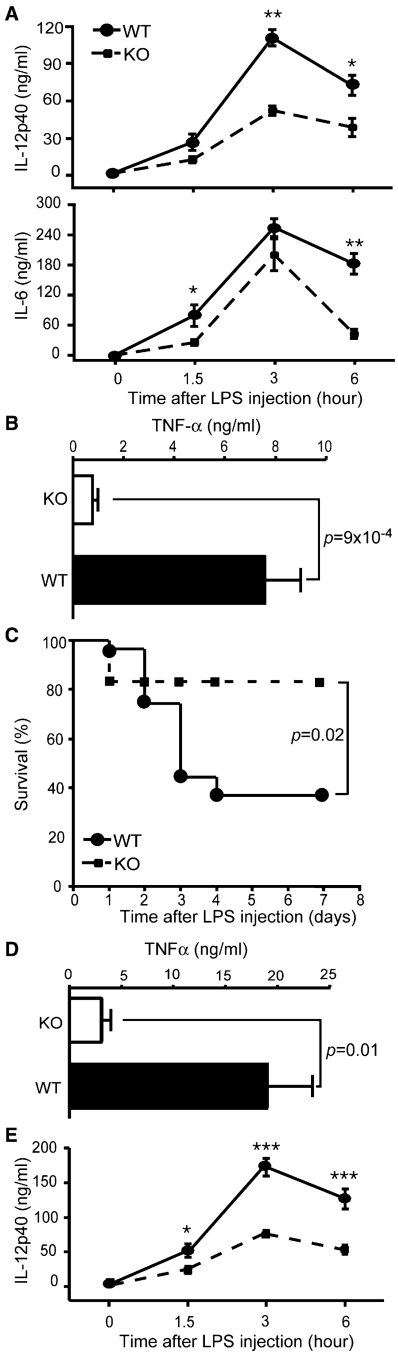


**Figure 5. Ablation of gp96 in Macrophages Results in Attenuation of Endotoxin Shock**

(A and B) 7-week-old KO mice (n = 5) or control littermates (n = 10) were administered i.p. with 0.5 mg LPS/mouse. Mice were bled at 0 (before LPS injection), 1.5, 3, and 6 hr after LPS injection. Serum IL-12p40 (A, top), IL-6 (A, bottom), and TNF-α (B) were quantified by ELISA. *p < 0.05; **p < 0.01. Two experiments were performed with similar findings.

(C) Survival curve of KO (n = 12) or WT (n = 27) mice after i.p. injection of 0.5 mg LPS/mouse.

(D and E) WT (n = 6) and KO (n = 5) mice were injected i.v. with 1 mg LPS/mouse, followed by measurement of serum TNF-α (D) and IL-12p40 (E).

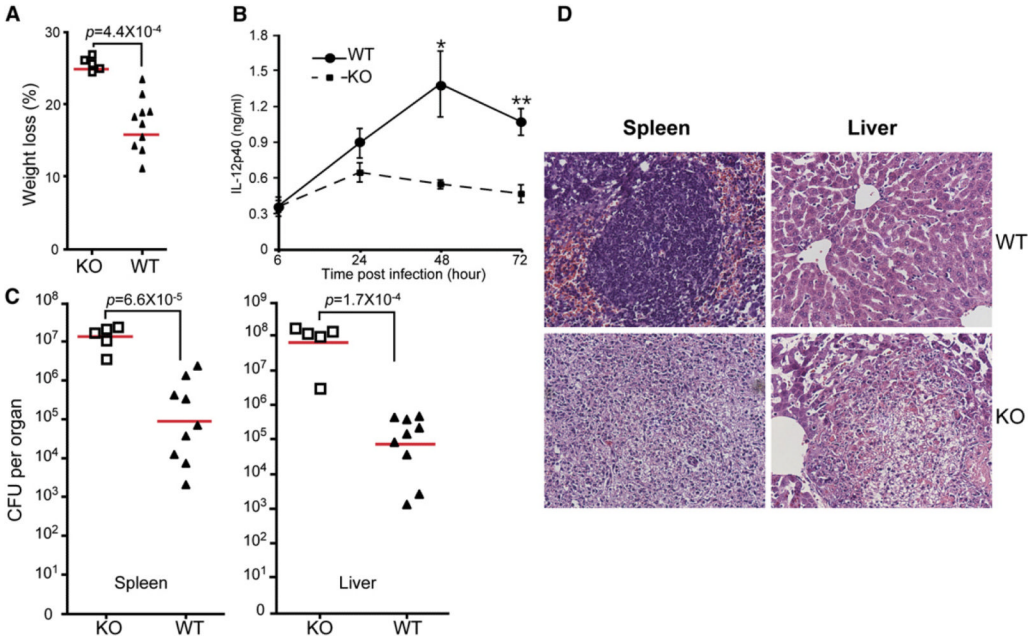


**Figure 6. LysMcre$^{+/-}$*Hsp90b1*$^{flox/-}$ Mice Are Highly Susceptible to *Listeria monocytogenes***

(A) Weight loss of mice 3 days after i.p. injection of *LmOVA* at 2 × $10^6$/mouse. Each symbol represents individual mouse.

(B) Mice in (A) were bled at 24, 48, and 72 hr after *LmOVA* injection. Serum IL-12p40 was measured by ELISA. *p < 0.05; **p < 0.01.

(C) *LmOVA*-infected mice were sacrificed 3 days after *LmOVA* injection. Bacteria load was measured. Symbols represent individual mice, and bars represent geometric mean of colony-forming unit (CFU)/organ.

(D) H&E-stained sections from infected mice at day 3 after infection. Section from one representative mouse per group is shown (magnification ×200).